

# Physical Adsorption of Block Copolymers to SWNT and MWNT: A Nonwrapping Mechanism

Einat Nativ-Roth,<sup>†</sup> Rina Shvartzman-Cohen,<sup>†</sup> Céline Bounioux,<sup>‡</sup> Marc Florent,<sup>†</sup>  
Dongsheng Zhang,<sup>§</sup> Igal Szleifer,<sup>§</sup> and Rachel Yerushalmi-Rozen<sup>\*,†,||</sup>

Department of Chemical Engineering, Ben-Gurion University of the Negev, 84105 Beer Sheva, Israel, The Jacob Blaustein Institute, Ben-Gurion University of the Negev, PO Box 653, Israel, Department of Chemistry, Purdue University, 560 Oval Drive, West Lafayette, Indiana 47907-2084, and The Ilse Katz Center for Meso- and Nanoscale Science and Technology, Ben-Gurion University of the Negev, 84105 Beer Sheva, Israel

Received March 4, 2007

**ABSTRACT:** A detailed study of the interaction mechanism between carbon nanotubes and physically adsorbed block copolymers is presented. The combination of experimental observations, computer simulations and theory suggests that while the solvophobic blocks adsorb to the nanotubes by a nonwrapping mechanism, the dangling (solvophilic) blocks provide a steric barrier that leads to the formation of stable dispersions of individual single walled carbon nanotubes (SWNT) and multiwalled carbon nanotubes (MWNT) above a threshold concentration of the polymer. The observed threshold concentration depends on the length of the solvophobic blocks, and it is higher for MWNT as compared to SWNT. Theory suggests that the latter is a consequence of dimensional considerations. Spectroscopic characterization of the dispersions indicate that the dispersing block polymers do not alter the electronic structure of the well dispersed individual SWNT, supporting the model of nonspecific adsorption of the polymer to the tube driven by van der Waals type interactions. The study presented here offers a generic scheme for optimization of the structure and composition of block copolymers used for dispersion of CNT in different media.

## Introduction

Carbon nanotubes (CNT) are graphitic structures with a typical diameter of 0.8–2 nm for single walled nanotubes (SWNT) and 10–40 nm for multiwalled nanotubes (MWNT) and a length of up to millimeters.<sup>1</sup> The novel structural mechanical and electronic properties of the individual tubes offer a promise to different fields of application including molecular electronics,<sup>2</sup> composite materials,<sup>3,4</sup> energy storage,<sup>5</sup> and biomedical applications.<sup>6</sup>

Yet, as-synthesized CNT are insoluble in aqueous and organic media. The individual tubes form ropes or bundles that contain up to 100 SWNT packed in a hexagonal lattice with an inter-tube distance comparable to the inter-sheet distance in graphite<sup>7</sup> (Figure 1).

Because of the high cohesion energy, SWNT of about 1  $\mu\text{m}$  long tubes experience a contact energy of  $40\,000\ k_{\text{B}}T$ ,<sup>8–10</sup> leading to the formation of bundles or ropes that further entangle into networks, as do MWNT. The large attractive interaction is short ranged and decreases to below  $k_{\text{B}}T$  within 2.5 nm (Figure 2).

Over the past few years a variety of methods were devised for exfoliation of SWNT bundles into individual tubes and dispersion the debundled tubes in different media.<sup>9</sup> The different strategies include chemical functionalization, covalent linking of monomers, oligomers or polymers,<sup>11</sup> complexation via  $\pi$ – $\pi$  interactions<sup>12,13,14</sup> adsorption of charged surfactants<sup>9,15,16</sup> and

wrapping by polymers.<sup>17–23</sup> While the range and strength of the resulting interactions depend on the chemical details of the system, a generic property of these methods is the disruption of the electronic structure of the dispersed tubes and some of their physical properties.<sup>24,25</sup> Among the *highly interventional* methods are covalent sidewall functionalization and wrapping by polyelectrolytes and conjugated polymers: In the case of covalent modification the translational symmetry of SWNT is disrupted by introducing  $\text{sp}^3$  carbon atoms, and the electronic and transport properties of the tubes are altered.<sup>26</sup> Wrapping of CNT may be driven by chemical interactions between the  $\pi$ -system of the CNT and the functional groups comprising the polymers: electrostatic interactions,  $\pi$ -stacking, and hydrogen bonding were found to dominate in different systems. It is now well accepted that polymer-wrapped CNT are strongly associating, tightly bound systems where the tube surface chemistry, electronic structure and the intrinsic inter-tube interactions are modified by the wrapping. Indeed, different studies which examined the electronic structure of tightly wrapped CNT by either synthetic conjugated polymers or biopolymers (DNA, peptides) suggest that a hybrid is formed where both the electronic properties of the polymer and the CNT are modified.<sup>27–35</sup>

An essentially different approach is presented below. Instead of aiming to attenuate the cohesion energy between tubes by reducing the short-ranged attraction, it is possible to utilize a relatively weak, but long ranged repulsion for creating a barrier that prevents the tubes from approaching the attractive region of the potential. It was shown that block copolymers may disperse CNT.<sup>8,9,36–41</sup> Block copolymers adsorption from selective solvent conditions may provide the osmotic (steric) repulsion<sup>42</sup> required for dispersing SWNT in aqueous and organic solvents. A motivation for this approach is the assumption that a weak interaction between the block copolymer and the SWNT

\* Corresponding author. Telephone: 972- 8-6461272. Fax: 972-8-6472916. E-mail: rachely@bgu.ac.il.

<sup>†</sup> Department of Chemical Engineering, Ben-Gurion University of the Negev.

<sup>‡</sup> The Jacob Blaustein Institute, Ben-Gurion University of the Negev.

<sup>§</sup> Department of Chemistry, Purdue University.

<sup>||</sup> The Ilse Katz Center for Meso- and Nanoscale Science and Technology, Ben-Gurion University of the Negev.

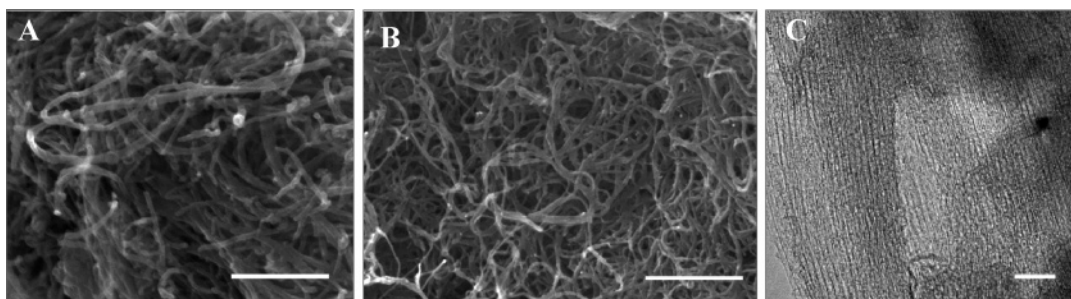


**Figure 1.** Scanning electron microscope (SEM) images of as-synthesized powders of (A) MWNT and (B) SWNT (Carbon Nanotechnology Inc, USA), scale bar 500 nm, and (C) high-resolution transmission electron microscope (HRTEM) image of SWNT, Nano Carblab (NCL), Russia, scale bar 10 nm.

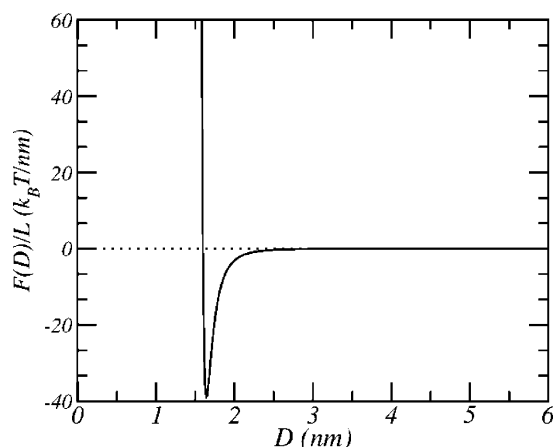


**Figure 2.** Interaction potential, per unit length, between two parallel SWNT as a function of the inter-tube distance. The potential was obtained from ref 10.

will not intervene with the electronic structure of the tubes. In Figure 3 we present the concept.

In previous studies, we focused on characterization of the properties of block copolymers–CNT dispersions and investigation of the dispersion mechanism.<sup>8, 9, 39</sup> Here we present a detailed study of the nature of the interaction between SWNT and the adsorbed polymer, investigate the effect of polymer bulk concentration on the formation of dispersions, and examine the applicability of this approach to dispersion of MWNT.

## Experimental Section

**Materials. Carbon Nanotubes (CNT).** SWNTAP was AP grade (Carbolex, University of Kentucky, Lexington, Kentucky). The nanotubes were synthesized by arc-discharge, and used as received. According to the specifications by the manufacturer, the as-prepared AP grade consists of 50–70 vol % SWNT. The samples contain graphite, carbon impurities and catalyst (cobalt and nickel, ca. 20 nm in diameter).

SWNTH was synthesized via the HiPco process<sup>44</sup> (Carbon Nanotechnology Inc, USA). Typical diameter was 1 nm and typical length of hundreds of nanometers to about 2  $\mu\text{m}$ .

MWNT produced by Catalytic Chemical Vapor Deposition were purchased from INP (Toulouse, France). The powder contains 95 vol % MWNT, typical tube diameters 10–20 nm and typical length in micrometers.

**Block Copolymers.** Two block copolymers soluble in organic solvents were used: Poly(styrene)–poly(methacrylic acid) diblock copolymer (PS–PMAA), where each PS block is of molecular weight 33 100 g/mol, and the PMAA block is of 6700 g/mol was purchased from Polymer Source Inc. Canada (P1861-SMAA, polydispersity index 1.1); poly(ethylene oxide-*b*- polydimethylsiloxane-*b*-ethylene oxide) triblock copolymer (PEO-*b*-PDMS-*b*-PEO), where each PEO block is of  $M_w$  2000 g/mol and the PDMS

block is of 12 000 g/mol. The polymer was kindly donated by M. Gottlieb.<sup>45</sup>

Different water-soluble Pluronics triblock copolymers were received as a gift from BASF AG Germany and used as received (Table 1).

**Solvents.** Analytical grade organic solvents were used: heptane, toluene, chloroform, *p*-xylene (Frutarom, Israel), and Millipore water ( $10^{18}$   $\Omega/\text{cm}$ ).

**Methods. Preparation.** Liquid dispersions were prepared by dissolving a block copolymer in a selective solvent (aqueous or organic) to form solutions of desired concentrations. The solutions were mixed for about 2–3 days using a magnetic stirrer or a roller. A powder of as-prepared nanotubes was sonicated at very mild conditions (50W, 43 kHz) for 1 h in the polymeric solution (these conditions were shown not to damage the tubes or the polymers).<sup>8,46</sup> Following the stage, the dispersions were centrifuged (at 4500 rpm for 30 min) and the supernatant was decanted from above the precipitate. SWNTH were sonicated for additional 2 h following 2–3 days incubation.

**Characterization. Morphological Characterization and Electron Microscopy (EM).** Ultrahigh resolution scanning electron microscopy (HRSEM) was used for imaging powders of as-prepared SWNT and MWNT. The dispersed CNT were characterized via direct imaging of the aqueous dispersions using cryo-transmission electron microscopy (cryo-TEM).<sup>47</sup> Dried samples were imaged using high-resolution transmission electron microscopy (HRTEM).

HRSEM measurements were carried out using A JSM-7400F (JEOL) ultrahigh resolution cold FEG-SEM. The apparatus allows the imaging of insulating materials without the need for coating the samples with a conducting coating.

Sample preparation for cryo-TEM measurements was carried out as follows: a drop of the solution was deposited on a TEM grid (300 mesh Cu grid) coated with a holey carbon film (Lacey substrate-Ted Pella Ltd). The excess liquid was blotted and the specimen was vitrified, by a rapid plunging into liquid ethane precooled with liquid nitrogen, in a controlled environment vitrification system. The samples were examined at  $-178$  °C using a FEI Tecnai 12 G<sup>2</sup> TWIN TEM equipped with a Gatan 626 cold stage, and the images were recorded (Gatan model 794 CCD camera) at 120 kV in low-dose mode. Samples for HRTEM imaging were prepared by placing a droplet of the dispersion on a TEM grid (300 mesh Cu, Ted Pella) and allowing the solvent to evaporate.

**Spectroscopic Characterization. UV–Vis Absorption and Raman Scattering.** UV–vis spectroscopy was carried out using a Jasco V-570 apparatus. Raman scattering studies were performed using a Jobin-Yvon LabRam HR 800 micro-Raman system, at a backscattering geometry. An excitation wavelength of 632.8 nm (HeNe laser), with spectral resolution of 4–8  $\text{cm}^{-1}$  was focused onto the sample surface through a 50 $\times$  objective lens.

**Simulation Methodology.** We performed molecular dynamics (MD) simulations to study the adsorption of F88 triblock copolymers, (PEO)<sub>100</sub>(PPO)<sub>64</sub>(PEO)<sub>100</sub>, on a capped (10,10) carbon nanotube of dimensions 1.328 nm  $\times$  1.328 nm  $\times$  21.142 nm. The simulations were carried out using the Gromacs 3.3.1<sup>48, 49</sup> software. The interactions potential for the pluronic block copolymers was obtained from the recently published coarse grained model of

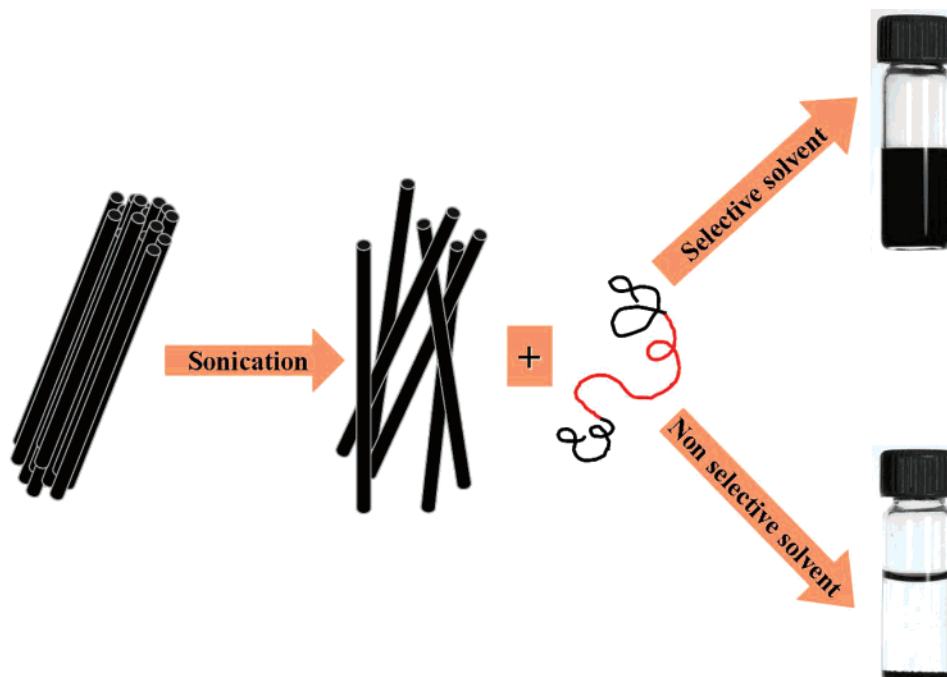


**Figure 3.** Block copolymers (designated A–B or A–B–A).<sup>43</sup> They are comprised of covalently linked incompatible moieties and disperse SWNT in selective solvents that act as a “good solvent” for one of the blocks (i.e., A),<sup>42</sup> while simultaneously acting as a “poor solvent” for the other block (B). Under these conditions polymer chains may adsorb via physical attachment of the B-block while the A blocks dangle into the solution repelling other polymer-decorated CNT and forming a long-lived dispersion. Nonselective solvents fail to disperse the SWNT.<sup>8,39</sup>

**Table 1. Composition of PEO–PPO–PEO Copolymers**

polymer	$M_w$	PEO wt %	product no.
F68	8400	80	583 097
P84	4200	40	586 440
F88	11 400	80	560 840
P103	4950	30	586 460
P104	5900	40	589 640
F108	14 600	80	583 062
P123	5750	30	587 440
F127	12 600	70	583 106

Bedrov et al.<sup>50</sup> and the force field for the carbon nanotube is a modified version of the one from Walther et al.<sup>51</sup> The nonbonded interactions between monomers in the copolymers and carbon in the nanotube were obtained by the Lorentz–Berthelot combination rules. The cutoff distance for all nonbonded interactions is 1.4 nm. We initiate the simulations by placing 10 triblock copolymers and the nanotube in a box of very large size. After the molecules become randomly distributed in the box, energy minimization is carried out to avoid large repulsive interactions. Then an *NVT*–MD simulation is performed at 300 K for 1 ns, with an integration step of 2 fs, using a Berendsen thermostat<sup>52</sup> with the coupling constant of 0.1 ps. Neighbor lists were utilized and updated every fifth integration step.

### Molecular Theory

The interactions between the polymer coated CNT’s and the chemical potentials of the adsorbed polymers is calculated using a molecular theory described in detail in refs 8 and 73. The basic idea is to consider each molecular species with all its intramolecular and surface interactions (polymer–nanotube) exactly, while the intermolecular interactions are determined approximately within a self-consistent approach. The theory has been shown to provide excellent quantitative agreement for the structure and thermodynamic properties of grafted polymer layers on surfaces of arbitrary geometry with full scale computer simulations<sup>53</sup> and with experimental observations.<sup>54,55</sup> The theory incorporates the detailed geometry and nanometric size of the tubes as well as the proper dimensions and conformations of the modeled PEO polymers.

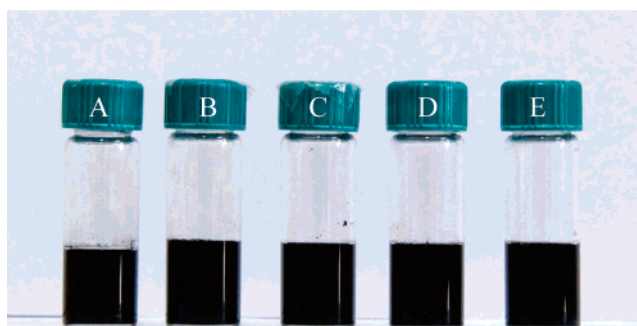


**Figure 4.** Dispersions of CNT (0.5 wt %) in polymeric solutions: (A) SWNTAP in 0.1 wt % F127 in water; (B) SWNTH in 0.5 wt % F127 in water; (C) SWNTH in 0.5 wt % PS–PMAA in chloroform; (D) MWNT in 1 wt % F68 in water; (E) MWNT in 1 wt % PEO-*b*-PDMS-*b*-PEO in heptane. Images were taken more than 2 months after preparation.

### Results

Images of the ink-like macroscopically homogeneous and stable dispersions are presented in Figure 4.

The microstructure of the dispersions was investigated using EM. In Figure 5, we present cryo-TEM images of SWNTAP (Figure 5A) and SWNTH (Figure 5B). Cryo-TEM is known to preserve the structures present in the bulk solution.<sup>47</sup> The images suggest that the dispersions are composed of individual SWNT, small bundles and catalyst particles. The length of the observed SWNT is well above 1  $\mu\text{m}$ .

In Figure 6, we present EM images of dispersions of MWNT. A cryo-TEM image provides an overview of the vitrified MWNT dispersion (Figure 6A) while Figure 6B presents an overview of the dried dispersion. A higher magnification reveals a double-walled CNT in close vicinity to another MWNT. We are unable to tell whether the structures on the tubes are amorphous carbon (as often seen in those samples)<sup>56</sup> or a dried polymer partially burnt under the electron beam.

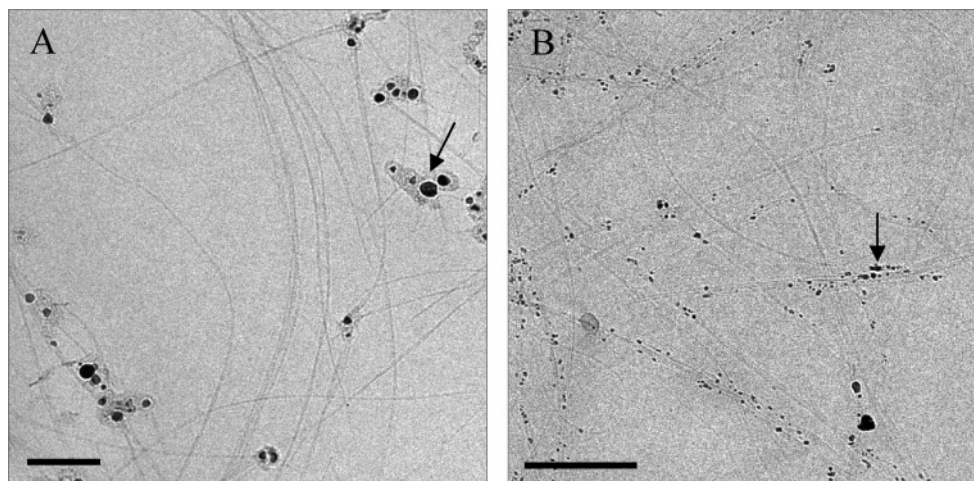


**Figure 5.** TEM micrographs of aqueous dispersions of SWNT. Cryo-TEM images of vitrified dispersion (A) 1 wt % of SWNTAP in 1 wt % F108; (B) 0.5 wt % SWNTH in 1 wt % F68. Scale bar = 100 nm. The arrows point to catalyst particles.

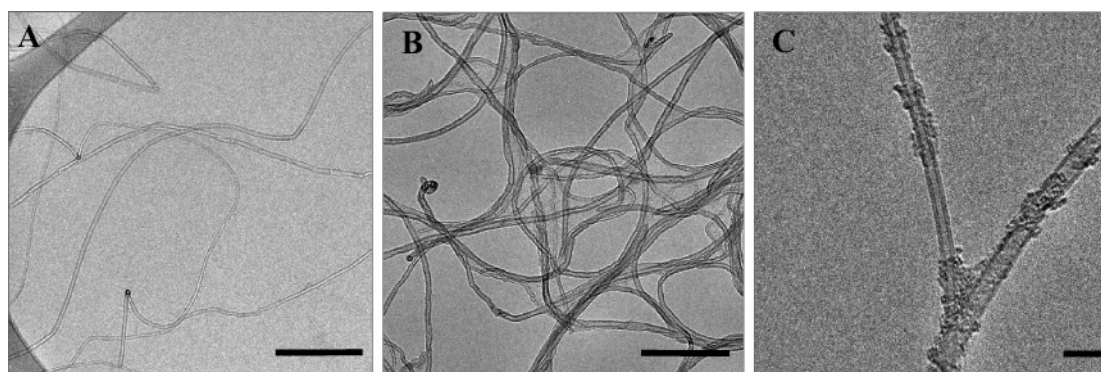


**Figure 6.** (A) Cryo-TEM image and (B) HRTEM image of a dried dispersion of 0.1 wt % MWNT (INP) in 0.25 wt % F127. Scale bar = 200 nm. (C) HRTEM image of a dried dispersion of 0.1 wt % MWNT (Cheap Tubes Inc., purity >90 wt %), in 1 wt % F108. Scale bar = 10 nm.

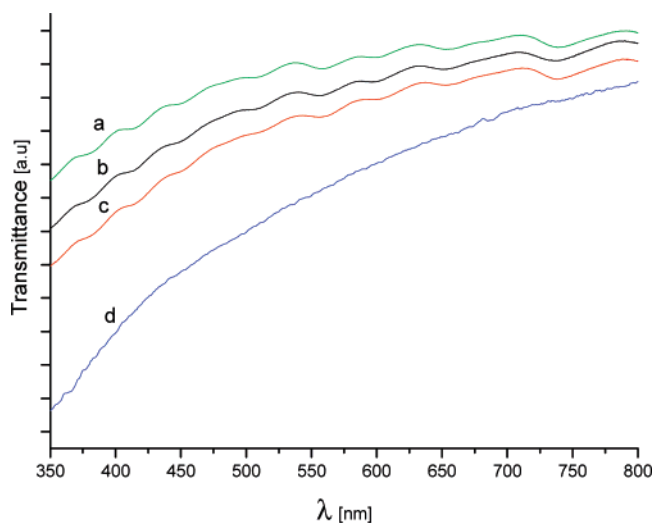


**Figure 7.** UV-vis absorption spectra of SWNTH (normalized and shifted along the vertical axis) in (a) toluene, (b) aqueous dispersion of Plurionics (F127, 0.5 wt %), (c) toluene dispersion in the block copolymer PS-PMAA, and (d) chemically modified SWNTH, courtesy of Wagner et al.<sup>58</sup>

The effect of the dispersing polymers on the electronic state of SWNT was investigated using UV-vis spectroscopy and Raman scattering. In Figure 7 we present UV-vis spectra of SWNTH dispersed in toluene, in solutions of a block copolymers and for comparison spectra of chemically modified SWNTH.<sup>57,58</sup> Theoretical modeling suggests that the molecular-like structure of CNT and the confinement in the circumferential direction

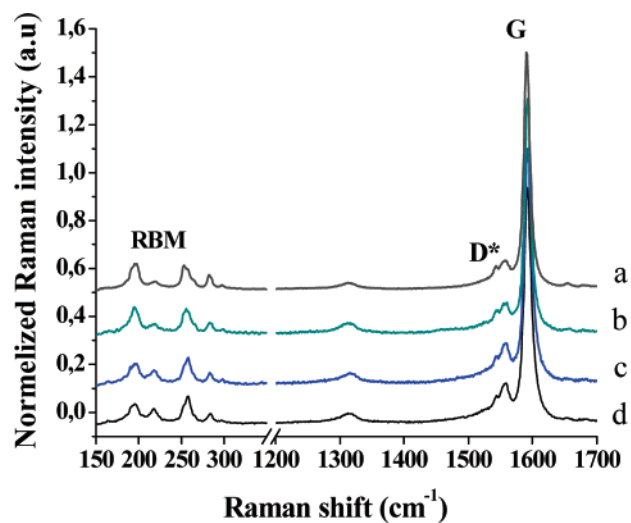


**Figure 8.** Raman spectra of SWNTH dispersed in (a) chloroform solution of PS-PMAA (0.2 wt %), (b) aqueous solution of P123 (1 wt %), and (c) aqueous solution of F127 (1 wt %) (d) and of the as-synthesized powder of SWNTH.<sup>59,60</sup>

lead to the clearly recognized van Hove singularities in the optical absorption UV-vis spectra of the dispersed SWNT, as indeed is observed in Figure 7.<sup>1,58</sup> Note that this is very different from the case of chemically functionalized tubes (Figure 7d), where localization of the  $\pi$ -electrons results in smoothing of the absorption spectra and the disappearance of the step-like structure.

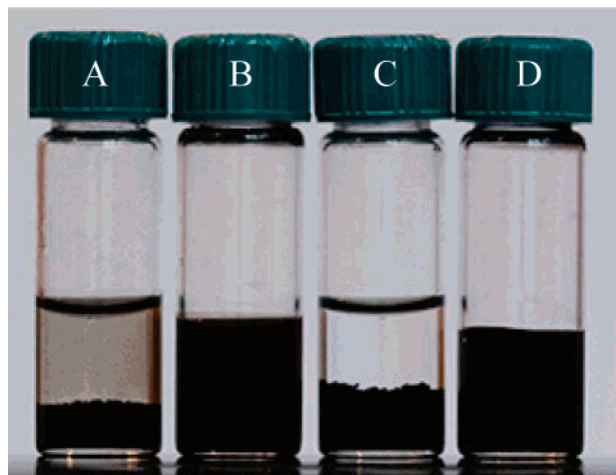


**Figure 9.** Aqueous dispersions of 0.1 wt % SWNTAP in (A) 0.05 wt % F127 and (B) 0.1 wt % F127 and of 0.1 wt % MWNT in (C) 0.075 wt % F127 and (D) 0.25 wt % F127.

Raman spectra of dried dispersions of SWNT are presented in Figure 8.

The spectral ranges of 150–350 and 1100–1700  $\text{cm}^{-1}$  are of interest.<sup>61</sup> The first interval is related to the radial breathing mode (RBM). In this range the position of the peak is sensitive to the excitation wavelength (here 632.8 nm). The RBM at 195 and 283  $\text{cm}^{-1}$  excitation indicate a resonant process occurring in SWNT with a narrow range of diameters around 0.80–1.25 nm, identified with transitions between van Hove singularities in the valence and conduction bands of semiconducting and metallic tubes respectively. The bands labeled G and D are found in the range 1100–1700  $\text{cm}^{-1}$ . The peak position of the D-band found in SWNT and in other graphitic lattices depends on the excitation energy, and its intensity correlates with defects in the SWNT structure.<sup>1,59,6</sup> In Figure 8, we observe that the intensity of the D band in the spectra of the dispersed SWNT has not changed with respect to the as-synthesized SWNT, unlike the case of functionalized SWNT, where a clear shift was reported.<sup>62</sup> Overall the Raman spectra indicates that the electronic structure of the SWNT is not modified in the dispersion process.<sup>59</sup> Similar results were obtained with a variety of block copolymers (PEO-*b*-PDMS-*b*-PEO, gum arabic, not presented).

We investigated the effect of polymer concentration in the bulk solution on the formation of stable dispersions in organic liquids of PS-PMAA and aqueous solutions of Pluronic. Following the procedure described above, SWNTAP, SWNT, and MWNT were sonicated in solutions of block copolymers of different concentrations and visually examined. Five sets of experiments were performed: (1) SWNTAP, (2) MWNT, sonicated in solutions of PS-PMAA in chloroform toluene and *p*-xylene; (3) SWNTAP; (4) MWNT; (5) SWNT sonicated in aqueous solutions of Pluronic triblock copolymer.

Apparently stable dispersions were centrifuged (at 4500 rpm for 30 min) and further incubated at room temperature for a few weeks, and designated as “stable” if agglomeration and phase separation were not observed. In a typical experiment concentrations of 0.05, 0.075, 0.1, 0.2, 0.5, 0.75, 1, and 2 wt % were prepared, and 0.1 wt % of the dry powder of CNT was added and the mixture sonicated. The resulting dispersions were centrifuged, followed by decantation of the supernatant from above the precipitate. The dispersions (supernatant) were incubated in room temperature and visually examined. Additional concentrations were examined when relevant. As

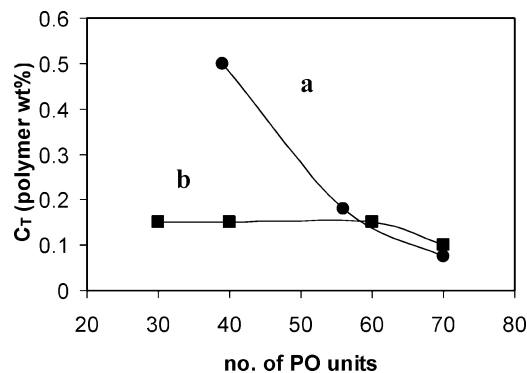


**Figure 10.** Threshold concentration ( $C_T$ ) for dispersions of 0.1 wt % SWNTAP by Pluronic triblock copolymers that differ by the length of the PEO block: (a) short PEO (P84, P103, P123) and (b) long PEO (F68, F88, F108, F127). The line is a guide to the eye.

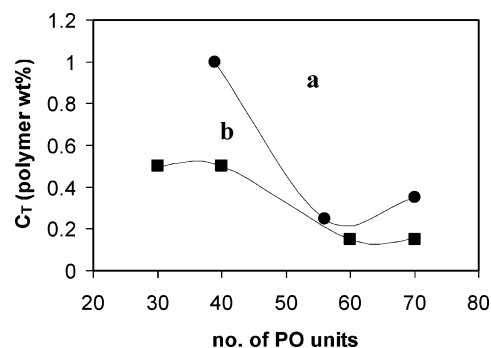


**Figure 11.**  $C_T$  for dispersions of 0.1 wt % MWNT by Pluronic triblock copolymers that differ by the length of the PEO block: (a) short PEO (P84, P103, P123) and (b) long PEO (F68, F88, F108, F127). The line is a guide to the eye.

**Table 2. Threshold Concentration ( $C_T$ ) Required for the Formation of a Stable Dispersion of CNT Using PS-PMAA in Different Solvents**

type of CNT (0.1 wt %)	solvent	$C_T$ (wt %)
SWNTAP	toluene	0.2
	chloroform	0.08
	<i>p</i> -xylene	0.1
MWNT	toluene	0.2
	chloroform	0.2
	<i>p</i> -xylene	0.15
SWNTH	chloroform	0.15

demonstrated in Figure 9, visual inspection enables one to discriminate between dispersed and nondispersed samples. The microscopic structure of the dispersions was examined using cryo-TEM (aqueous solutions) and HRTEM (aqueous and organic solutions) (Figures 5 and 6).

In Tables 2 and 3, we summarize the results.

We found that for the examined polymers there exists a minimal polymer concentration, necessary for the formation of stable dispersions of SWNT and MWNT. At this concentration, the dispersion is stable, and agglomeration does not take place following centrifugation, separation of the initial precipitate from the supernatant, and prolonged incubation. Typical threshold concentrations are in the range of 0.1–0.2 wt %.

For the Pluronic series, we examined the dependence of the value of  $C_T$  on the composition and molecular weight of the polymer.

In Figure 10, we present  $C_T$  for SWNTAP in aqueous solutions of Pluronic as a function of the number of the PO segments (the hydrophobic block). The two series are distinguished by the number of the EO segments which is 17–20 (a)

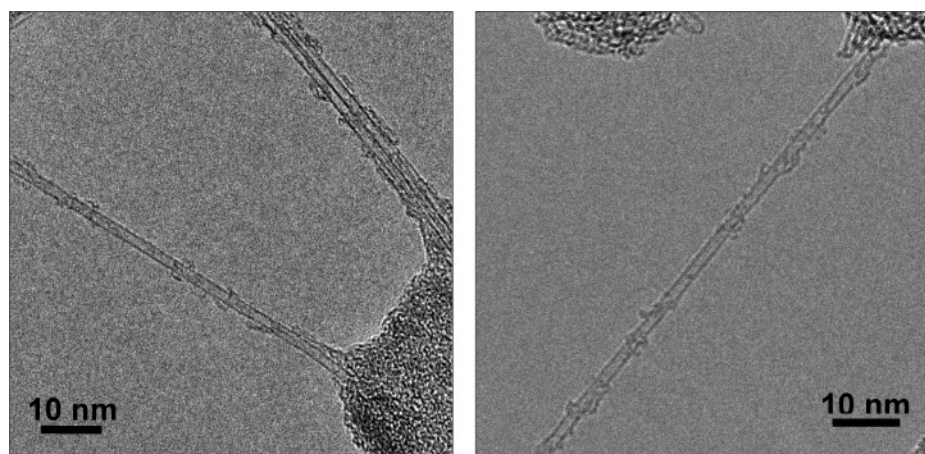


**Figure 12.** HRTEM image of a dried dispersion of SWNTAP prepared by dilution of a dispersion in F127 (0.15 wt %) to a final concentration of 0.035 wt %.

**Table 3. Threshold Concentration ( $C_T$ ) Required for the Formation of a Stable Dispersion of 0.1 wt % CNT in Pluronic Block Copolymers**

	polymer	$M_w$	no. of PO units	no. of EO units (for each of the blocks)	$C_T$ (wt %) SWNTAP	$C_T$ (wt %) MWNT	cmc (wt %, 25 °C)
short PEO	P84	4200	39	17	0.5	1	2.6 <sup>65</sup>
	P103	4950	56	16	0.18	0.25	0.36 <sup>64</sup>
	P123	5750	70	20	0.08	0.5	0.004, <sup>64</sup> 0.03 <sup>63,65</sup>
long PEO	F68	8400	30	80	0.15	0.5	1.2 <sup>56</sup>
	F88	11 400	40	100	0.15	0.5	0.5 <sup>64</sup>
	F108	14 600	60	130	0.15	0.15	4, <sup>66</sup> 4.5 <sup>65</sup>
	F127	12 600	70	106	0.1	0.25	0.7, <sup>65</sup> 1, <sup>67</sup> 4.2 <sup>68</sup>

<sup>a</sup> We note here that the reported cmc values of Pluronic are characterized by a large variability.

and about 110 ( $\pm 20$ ) in (b). We observe a clear tendency of reduction in  $C_T$  with increasing length of the PPO chain (within a series, i.e., for a given PEO length). We also observe that an overall lower bulk concentration is required for formation of stable dispersions of SWNT when the PEO chain is longer, as was observed before.<sup>38</sup> Both series converge at F127 and P123.

The results reported in Figures 10 and 11 were repeated with a few different types of SWNT and MWNT, giving similar results. The results for SWNT are presented in the Supporting Information.

In Figure 11, we present  $C_T$  for dispersion of MWNT in aqueous solutions of Pluronic. Again, two series which differ in the length of the PEO block are presented. Along each series the length of the PPO block increases, as in Figure 10. We observe a similar tendency to that presented in Figure 10: overall a longer PEO block (for a similar length of the PPO block) results in a lower threshold concentration while for a given PEO length the longer PPO results in a lower threshold concentration. Note that overall, the threshold concentration is significantly higher for MWNT than for SWNT. We relate to this point in the discussion.

The issue of adsorption reversibility is important both for the understanding of the adsorption mechanism and for practical consideration. To test the reversibility of adsorption, we carried out the following experiment: 0.1 wt % SWNTAP powder was dispersed in a solution of F127 at a polymer concentration of 0.15 wt %. This concentration is just above the minimal polymer concentration required for dispersion (as indicated in Table 3). A stable dispersion was obtained. The dispersion was then diluted in water resulting in a final polymer concentration of 0.035 wt %. The diluted dispersion remained macroscopically stable for a few weeks, and HRTEM image indicated that the dispersed moieties are individual tubes (Figure 12). Note that

this concentration is below the threshold concentration, and indeed when SWNT powder was sonicated in a solution of F127 of this concentration a dispersion did not form. Similar results were obtained for other Pluronic. In a different experiment, we dialyzed the dispersions through a membrane, allowing solvated polymer to diffuse out of the dialyzed reservoir. We found that in some cases dialysis resulted in agglomeration of the dispersion. The agglomerated dispersions could be redispersed by addition of free polymer and resonication.

## Discussion

Block copolymers were shown to be an efficient tool for dispersing CNT in aqueous and organic liquids.<sup>9</sup> The dispersing block copolymers may be further used for shear alignment of the dispersed CNT,<sup>69</sup> preparation of CNT-polymer composites where the block copolymers serve as compatibilizing agents,<sup>70</sup> adhesion promoters, and coupling agents<sup>71,72</sup> and as a targeting agent for SWNT assembly at interfaces.<sup>73</sup> Two modes of interaction between dispersing polymers and CNT suggested in the literature include strongly associated structures described by the “wrapping” model<sup>17–23</sup> and polymer-decorated CNT (a non-“wrapping” model).<sup>8,9</sup> Essentially, the two models differ in the degree of coupling between the polymers and the CNT. While the wrapping model suggests the existence of strong interactions that highly intervene with the electronic structure of both the polymer and the CNT, the nonwrapping model assumes that the polymer-tube interactions are nonspecific, restricted to the adsorbing block (or end group) and thus do not intervene with the electronic structure of the tubes or modify their physical properties.

In Figure 13, we present a snapshot from the MD simulations describing a case of nonwrapping. The figure is taken from a molecular dynamics simulation of the adsorption of pluronic

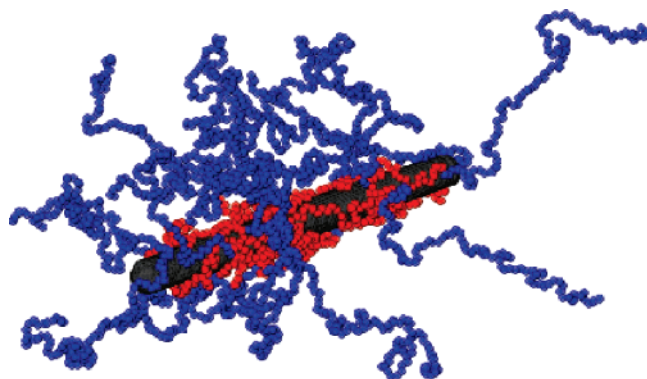


**Figure 13.** Snapshot from a molecular dynamics simulation of F88 and a CNT. The red spheres represent the PO groups while the blue spheres represent the EO segments.

F88 on a SWNT. The figure shows the typical state of the triblocks after adsorbing on the surface of the nanotubes from a bulk solution. Lack of structure is clearly observed in the adsorbed PPO blocks (red beads). Furthermore, the PEO blocks are not adsorbed but are rather tethered via the PPO block. The formation of a tethered polymer layer is the origin of the repulsive interactions leading to the dispersion of the tubes; see below.

In accordance with the picture presented above, the UV–VIS and Raman spectroscopy data presented in this study indicate that the dispersing polymers do not modify the electronic structure of the dispersed CNT, as expected from nonspecific physical adsorption (vdW interactions).

The configuration of amphiphilic block polymers in dispersions of SWNT was previously investigated by Dror et. al using small-angle neutron scattering (SANS).<sup>74,75</sup> In a quantitative study they found that scattering data from stable polymeric dispersions of SWNT were consistent with the formation of individual and small bundles (of about 3–4 tubes) of SWNT decorated by polymeric coils loosely adsorbed to the nanotubes surface. In particular, the scattering data could not be fitted to the  $-1$  power law that is consistent with a tight wrapping model.<sup>74</sup> The adsorbed polymers retained their coil-like configuration and the typical radius of gyration, exhibiting the typical scattering pattern expected from the structure presented in Figure 13.

In previous studies, we presented detailed modeling of the steric barrier formed by end-attached PEO layers. We showed that the strength and range of the steric repulsions induced by the polymers are monotonic increasing functions of both the chain length and polymer surface coverage.<sup>8,9</sup> In the present study, we show (Figure 14) a particular example where repulsion is induced by the presence of PEO dangling tails between two parallel CNT each with a coverage similar to the snapshot presented in Figure 13. The solid line represents the repulsions induced by the polymers and the dashed line is the total effective interaction between the tubes. While there is still a very large attraction at short distances, the polymer layer presents a very large barrier, on the order of  $10k_B T/nm$  at an inter-tube separation of 2.5 nm. As was discussed before,<sup>8,9</sup> the very short range of the inter-tube attractive potential, originating from the nanometric diameter of the tubes and their hollow structure, renders relatively short polymers effective stabilizers for SWNT. The experimental results (Table 3) indicate that PEO chains of about 20 monomers are already sufficient for dispersing CNT. Calculations of the polymer induced repulsive interactions (results not shown and refs 8 and 9) indicate that while the repulsions increase with polymer molecular weight and surface

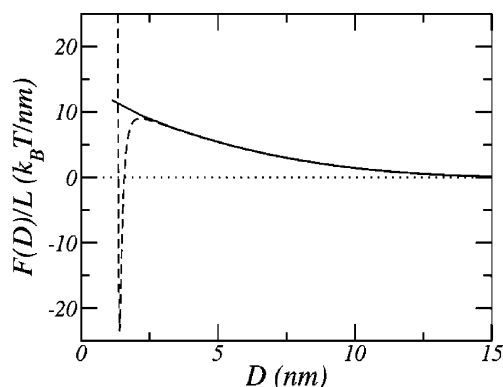


**Figure 14.** Polymer-induced repulsion (solid line) and the total potential (dashed line) between two parallel CNT coated with pluronic F88. The calculations were carried out using the molecular theory for the tethered PEO blocks. The surface density of PEO is  $1/3 \text{ nm}^{-2}$ . The total potential is obtained by adding the repulsive interactions with the bare CNT attractions shown in Figure 1.

coverage, short chains will induce a sufficiently large repulsion to stabilize the SWNT. In general terms, a barrier of  $5k_B T/nm$  would probably be enough to stabilize and disperse individual CNT. The calculations presented in Figure 14, and in more detail in refs 8,9 provide guidelines for the minimal molecular weight of each of the blocks that would lead to the formation of stable dispersions of CNT.

In this study, we found that the dispersing efficiency of different block copolymers as indicated by threshold block copolymers concentration  $C_T$  (Tables 2 and 3), depends on the structure and composition of the block copolymer, the solvent and the dispersed moiety (MWNT vs SWNT). A systematic study of the dependence of  $C_T$  on the composition of the block copolymer, and the adsorption mechanism was carried out for the Pluronic series. The results presented in Table 3 indicate that apart from the case of P123,  $C_T$  is reached below the cmc values of the native Pluronic solution, suggesting that the stabilization of SWNT and MWNT occurs via single-chain adsorption, in line with the concept presented above (Figures 13 and 14).

What is the origin of the observed dependence of  $C_T$  on the length of the PPO block? It is well-known<sup>76</sup> that in polymer-stabilized dispersions the configuration of the adsorbed polymers, the thermodynamic state and the properties of the dispersion depend on the interaction between the adsorbing block and the dispersed moiety. The structure obtained by the MD simulations, (Figure 13), suggests that all (or most) of the PO segments are adsorbed to the CNT. Thus, the total free energy of adsorption at the saturation point should show a linear dependence on the length of the PPO block, for a fixed PEO length. Consequentially, a longer hydrophobic block is expected to result in a larger adsorbed amount, up to a length of the PPO block above which the adsorption reaches saturation (the adsorption plateau).<sup>77,78</sup> The configuration presented in Figure 13 implies as well that the strength of the PO segment–CNT interactions is on the order of the thermal energy (as expected from the hydrophobic nature of the PPO block and that of the CNT). It is important to emphasize that this vdW-type interaction does not modify the electronic properties of the nanotubes (unlike chemical functionalization).

We note that the experimentally observed  $C_T$  is not necessarily identical to the adsorption plateau. Rather it corresponds to the bulk concentration of the polymer necessary for achieving a surface concentration that would present a large enough steric barrier for dispersion of CNT. Namely, the concentration of

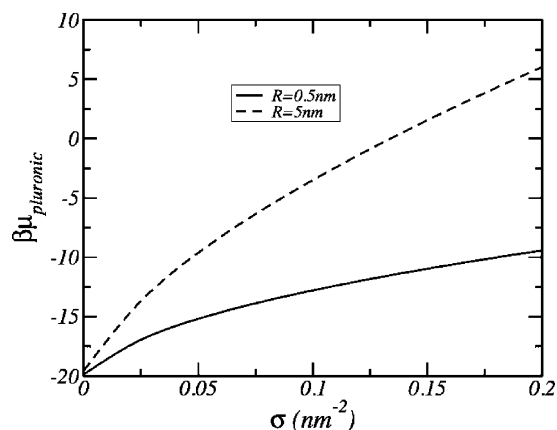


**Figure 15.** Chemical potential of the PEO blocks of pluronic chains adsorbed on the surface of nanotubes as a function of the adsorbed amount per unit area ( $\sigma$ ). The two curves correspond to different radius of the tube corresponding to SWNT ( $R = 0.5$  nm) and MWNT ( $R = 5.0$  nm). The calculations were carried out using the molecular theory.

polymer at which the adsorption will create a high-enough steric barrier (Figure 14). As longer PPO blocks, at fixed PEO length, increase the adsorbed amount, they lower the bulk concentration of pluronic sufficient for formation of a barrier high enough to induce dispersion. Thus, the experimentally observed lower  $C_T$  value for the longer PPO moieties results from the achievement of surface density enabling dispersion at a lower bulk concentration.

There are several important trends in the variation of  $C_T$  with PPO length, PEO length and the dispersed moiety (single vs multiwalled nanotubes). All are related to the adsorption of the triblock copolymer and to the dependence of the adsorption on molecular parameters, in particular chain length of the blocks. As we have discussed above the adsorption of the block copolymer increases with the length of the PPO segment, and therefore we observe a decrease of  $C_T$  with PPO length. The effect is very pronounced for short PEO blocks and very weak for the longer PEO studied here.

The origin of the PEO-length dependence was discussed by us (and by others<sup>38</sup>) before where we have shown that for a fixed surface coverage the longer PEO block generates a higher steric barrier between approaching CNTs, and therefore is able to disperse CNT at a smaller surface concentration.<sup>8,9</sup> Thus, shorter PEO blocks require a higher adsorption and therefore a larger bulk concentration (for a fixed length of the PPO block). Note that the relation between the bulk concentration and the adsorbed amount should decrease as the length of the PPO increases, as adsorption becomes more favorable.

While the effect of the PEO block-length on the adsorption is in accordance with the conclusions of Moore et al.,<sup>38</sup> the dependence on the length of the PPO block contradicts their conclusion that the PPO block does not play a significant role in the dispersion ability of Pluronic block copolymers.

Another interesting observation is the much larger value of  $C_T$  required for dispersion of MWNT as compared to SWNT. Here again we believe that the phenomenon results from the geometry and dimensions of the dispersed species: SWNT and MWNT differ by their diameter. Thus, a similar number of adsorbed chains would result in a lower surface density for the MWNT. This is quantified in Figure 15 where the chemical potential of two different pluronics adsorbed on SWNT and MWNT are shown as a function of the adsorbed polymers density (chains per square nanometers). The chemical potentials presented in the figure were calculated using the theory used to determine the interaction between polymer coated nanotubes

shown in Figure 14. A random organization of the PPO block on the surface was assumed, in line with the simulation results presented in Figure 13. The total chemical potential of the adsorbed pluronic is obtained by adding to the curves shown the value  $N_{\text{PPO}} \chi_{\text{ps}}$  where  $\chi_{\text{ps}}$  is the strength of a PO segment-CNT surface attraction. We estimate its value to be around  $1.0 k_B T$ . However, the exact number is irrelevant since the contribution of the PPO is independent of polymer surface coverage. Therefore, for each pluronic it adds a constant to the chemical potential.

The bulk concentration of the polymer determines the chemical potential. As observed from the graph, the adsorbed amount per unit area, for fixed chemical potential, is much higher for SWNT than for MWNT (with typical values of 4–5 chains /nm<sup>2</sup> for SWNT (see TGA data in the Supporting Information)). The complementary argument would suggest that to achieve a fixed surface density of polymer, the chemical potential in the MWNT has to be larger, corresponding to a higher bulk concentration of polymer. This is the origin of the consistently higher values of  $C_T$  observed in dispersions of MWNT vs SWNT.

Another important consequence of the polymeric nature of the adsorbing species is the irreversibility of adsorption toward finite dilution. The latter was observed as well by Park et al.<sup>26</sup> It is well-known that even when monomers adsorb and desorb reversibly long chains adsorb irreversibly, where in the limit of infinite length, polymer chains remain adsorbed to a surface even at zero bulk concentration. The origin of that behavior is the desorption mechanism: desorption of a chain requires coordinated removal of all the monomers, and the probability for that is negligible even for rather short chains. The dialysis experiments performed by us suggest that indeed some desorption takes place at extreme dilution, setting the limits of stability for dilution of the investigated dispersions.

## Conclusions

We found that dispersion of SWNT via steric repulsion among physically adsorbed (non wrapping) block copolymers is applicable to SWNT as well as MWNT. Spectroscopic characterization of dispersed SWNT indicates that the dispersing block polymers do not alter the electronic properties of the well dispersed SWNT. A threshold polymer concentration necessary for formation of stable dispersions is higher for MWNT was found to depend (for a given length of the non-adsorbing moiety) on the length of the adsorbing moiety. While analysis suggests that our observations are generic, and result from the nanometric dimensions of the CNT, we expect that the actual value of the threshold concentration would depend on the detailed surface composition of the CNT resulting from the synthesis method, surface treatment, purification process. These affect the surface energy of CNT and often result in residual surface groups that alter the details of the interaction. The analysis presented above may serve for optimization of the structure and composition of block copolymers used for dispersion of CNT in different media, where one can chose between a long tail and a long adsorbing moiety, according to the needs presented in different applications of CNT.

At the fundamental level, the study presented here demonstrates the important role played by the nanometric size of the tubes. This is manifested, for example, in the very large variations in the adsorption of polymers by moving from SWNT to MWNT. These results emphasize the importance in considering the detailed structures of the systems as the surface curvature of the tubes is of the same order of magnitude as a small number of segments of the polymer.



**Acknowledgment.** We thank D. Wagner for providing us with the spectra of the functionalized SWNT (Figure 7(d)). R.Y.-R. would like to thank the Israel Science Foundation, (Grant No.512/06). R.Y.-R. and I.S. are grateful to the BSF-United States-Israel Binational Science Foundation for supporting the cooperation leading to the development of some of the concepts presented in this work. I.S. thanks the NSF for partial support of this work. D. Z. thanks Prof. Bedrov for providing the potentials from ref 50.

**Supporting Information Available:** Text discussing the determination of the threshold concentration of SWNT in Pluronic solutions and an investigation of the TGA behavior of the dispersions, which was used to calculate the adsorbed amount of Pluronic, a table of threshold concentrations, and figures showing a plot of the threshold concentrations and mass change as a function of temperature. This material is available free of charge via the Internet at <http://pubs.acs.org>.

## References and Notes

- Dresselhaus, M. S.; Dresselhaus, G.; Avouris, Ph., Eds. *Carbon Nanotubes; Topics in Applied Physics 80*; Springer-Verlag: Berlin and Heidelberg, Germany, 2001.
- Joachim, C.; Gimzewski, J. K.; Aviram, A. *Nature (London)* **2000**, *408*, 541–548.
- Ajayan, P. M.; Charlier, J. C.; Rinzler, A. G. *Proc. Natl. Acad. Sci. U.S.A.* **1996**, *96*, 14199.
- Baughman, R. H.; Zakhidov, A. A.; de Heer, W. A. *Science* **2002**, *297*, 792 and references therein.
- Niu, C.; Sichel, E. K.; Hoch, R.; Moy, D.; Tennent, H. *Appl. Phys. Lett.* **1997**, *70*, 1480.
- Chen, X.; Lee, G. S.; Zettle, A.; Betoizzi, C. R. *Angew. Chem., Int. Ed.* **2004**, *43*, 6111.
- Thess, A.; Lee, R.; Nikolaev, P.; Hongjie, D.; Petit, P.; Robert, J.; Xu, C.; Lee, Y. H.; Kim, S. G.; Rinzler, A. G.; Colbert, D. T.; Scuseria, G. E.; Tománek, D.; Fischer, J. E.; Smalley, R. E. *Science* **1996**, *273*, 483.
- Shvartzman-Cohen, R.; Nativ-Roth, E.; Baskaran, E.; Levi-Kalisman, Y.; Szeleifer, I.; Yerushalmi-Rozen, R. *J. Am. Chem. Soc.* **2004**, *126*, 14850–14857.
- Szeleifer, I.; Yerushalmi-Rozen, R. *Polymer* **2005**, *46*, 7803.
- Girifalco, L. A.; Hodak, M.; Lee, R. S. *Phys. Rev. B* **2000**, *62*, 13104.
- Tasis, D.; Tagmatarchis, N.; Georgakilas, V.; Prato, M. *Chem.—Eur. J.* **2003**, *9*, 4000–4008.
- Chen, R. J.; Zhang, Y.; Wang, D.; Dai, H. *J. Am. Chem. Soc.* **2001**, *123*, 3838.
- Zhm, W.; Minami, N.; Kazaoui, S.; Kim, J. *J. Mater. Chem.* **2004**, *19*, 1924.
- Chen, J.; Liu, Y.; Weimer, W. A.; Halls, M. D.; Waldeck, D. H.; Walker, G. C. *J. Am. Chem. Soc.* **2002**, *124*, 9034–9035.
- Vigolo, B.; Penicaud, A.; Coulon, C.; Sauder, C.; Paillet, R.; Journet, C.; Bernier, P.; Poulin, P. *Science* **2000**, *290*, 1331.
- Wang, H.; Zhou, W.; Ho, D. L.; Winey, K. I.; Fischer, J. E.; Glinka, C. J.; Hobbie, E. K. *Nano Lett.* **2004**, *4*, 1789–1793.
- Steuerman, D. W.; Star, A.; Narizzano, R.; Choi, H.; Ries, R. S.; Nicolini, C.; Stoddart, J. F.; Heath, J. R. *J. Phys. Chem. B* **2002**, *106*, 3124.
- Rouse, J. H. *Langmuir* **2005**, *21*, 1055–1061.
- Chou, S. G.; Ribeiro, H. B.; Barros, E. B.; Santos, A. P.; Neizch, D.; Samsonidze, G. G.; Fantini, C.; Pimenta, M. A.; Jorio, A.; Filho, F. P.; Dresselhaus, M. S.; Dresselhaus, G.; Saito, R.; Zheng, M.; Onoa, G. B.; Semke, E. D.; Swan, A. K.; Unlu, M. S.; Goldberg, B. B. *Chem. Phys. Lett.* **2004**, *397*, 296–301.
- Dieckmann, G. R.; Dalton, A. B.; Johnson, P. A.; Razal, J.; Chen, J.; Giordano, G. M.; Munoz, E.; Musselman, I. H.; Baughman, R. H.; Draper, R. K. *J. Am. Chem. Soc.* **2003**, *124*, 1770.
- O'Connell, M. J.; Boul, P.; Ericson, L. M.; Huffman, C.; Wang, Y.; Haroz, E.; Kuper, C.; Tour, J.; Ausman, K. D.; Smalley, R. E. *Chem. Phys. Lett.* **2001**, *342*, 265.
- Star, A.; Steuerman, D. W.; Heath, J. R.; Stoddart, F. *Angew. Chem., Int. Ed.* **2002**, *41*, 2508.
- Baskaran, D.; Mays, J. M.; Bratcher, M. S. *Chem. Mater.* **2005**, *17*, 3389–3397.
- Jorio, A.; Pimenta, M. A.; Souza, A. G.; Filho, R. Dresselhaus, G.; Dresselhaus, M. S. *New J. Phys.* **2003**, *5*, 139.1–139.
- Baibarac, M.; Baltog, I.; Mihut, L.; Preda, N.; Velula, T.; Godon, C.; Mavellec, J. Y.; Werv, J.; Lefrant, S. *J. Optoelectron. Adv. Mater.* **2005**, *74*, 2173–2181.
- Park, H.; Zhao, J.; Lu, J. P. *Nano Lett.* **2006**, *6*, 916–919.
- McCarthy, B.; Coleman, J. N.; Czerw, R.; Dalton, A. B.; Panhuis, M. I. H.; Maiti, A.; Drury, A.; Bernier, P.; Nagy, J. B.; Lahr, B.; Byrne, H. J.; Carroll, D. L.; Blau, W. J. *J. Phys. Chem. B* **2002**, *106*, 2210–2216.
- Dalton, A. B.; Blau, W. J.; Chambers, G.; Coleman, J. N.; Henderson, K.; Lefrant, S.; McCarthy, B.; Stephan, C.; Byrne, H. J. *Synth. Met.* **2001**, *121*, 1217.
- Star, A.; Stoddart, F.; Steuerman, D.; Diehl, M.; Boukai, A.; Wong, E. W.; Sung-Wook, C.; Hyeon, C.; Heath, J. R. *Angew. Chem., Int. Ed.* **2001**, *409*, 1721.
- Steuerman, D. W.; Star, A.; Narizzano, R.; Choi, H.; Ries, R. S.; Nicolini, C.; Stoddart, J. F.; Heath, J. R. *J. Phys. Chem. B* **2002**, *106*, 3124.
- Rouse, J. H. *Langmuir* **2005**, *21*, 1055–1061.
- Ago, H.; Petritsch, K.; Shaffer, M. S. P.; Windle, A. H.; Friend, R. H. *Adv. Mater.* **1999**, *11*, 1281–1283.
- Cheng, F. Y.; Adronov, A. *Chem.—Eur. J.* **2006**, *12*, 5053–5059.
- Wang, D.; Ji, W. X.; Li, Z. C.; Chen, L. W. *J. Am. Chem. Soc.* **2006**, *1284*, 6556–6557.
- Yuan, W. Z.; Sun, J. Z.; Dong, Y.; Haussler, M.; Yang, F.; Xu, H. P.; Zin, A.; Lam, W. Y.; Zheng, Q.; Tang, B. Z. *Macromolecules* **2006**, *39*, 8011–8020.
- Duro, R.; Souto, C.; Gomez —Amoza, J. L.; Concheiro, R. A. *Drug. Dev. Ind. Pharm.* **1999**, *25*, 817–829.
- Bandyopadhyaya, R. Nativ-Roth, E.; Regev, O.; Yerushalmi-Rozen, R. *Nano Lett.* **2002**, *2*, 25.
- Moore, V. C.; Strano, M. S.; Haroz, E. H.; Hauge, R. H.; Smalley, R. E.; Schmidt, J.; Talmon, Y. *Nano Lett.* **2003**, *3*, 1379.
- Shvartzman-Cohen, R.; Levi-Kalisman, Y.; Nativ-Roth, E.; Yerushalmi-Rozen, R. *Langmuir* **2004**, *20*, 6085.
- Block copolymers may also disperse CNT by encapsulating them within micelles, see: Shin, Hye-in.; Min, B. G.; Jeong, W.; Park, C. *Macromol. Rapid Commun.* **2005**, *26*, 1451–1457.
- Kang, Y.; Taton, T. A. *J. Am. Chem. Soc.* **2003**, *125*, 5650.
- Napper, D. H., Ed. *Polymeric Stabilization of Colloidal Dispersions*; Academic Press, Inc.: Orlando FL, 1993.
- Hadjichristidis, N.; Pispas, S.; Floudas, G. *Block Copolymers: Synthetic Strategies, Physical Properties, and Applications*; John Wiley & Sons Europe: London, 2003.
- Nikolaev, P.; Bronikowski, M. J.; Bradley, R. K.; Rohmund, F.; Colbert, D. T.; Smith, K. A.; Smalley, R. E. *Chem. Phys. Lett.* **1999**, *313*, 91.
- Zhang, Z. R.; Gottlieb, M. *Thermochim. Acta* **1990**, *336*, 133.
- Strano, M. S.; Moore, V. C.; Miller, M. K.; Allen, M. J.; Haroz, E. H.; Kittrell, C.; Hauge, R. H.; Smalley, R. E. *J. Nanosci. Nanotech.* **2003**, *1*, 81.
- Talmon, Y. In *Cryo techniques in biological electron microscopy*; R.A. Steinbrecht, K. Zierold Eds.: Springer-Verlag: Berlin, 1987.
- Berendsen, H. J. C.; van der Spoel, D.; van Drunen, R. *Comp. Phys. Comm.* **1995**, *91*, 43–56.
- Lindahl, E.; Hess, B. A. an der Spoel, D. *J. Mol. Mod.* **2001**, *7*, 306–317.
- Bedrov, D.; Ayyagari, C.; Smith, G. D. *J. Chem. Theory Comput.* **2006**, *2*, 598–606.
- Walther, J. H.; Jaffe, R.; Halicioglu, T.; Koumoutsakos, P. *J. Phys. Chem. B* **2001**, *105*, 9980–9987.
- Berendsen, H. J. C.; Postma, J. P. M.; DiNola, A.; Haak, J. R. *J. Chem. Phys.* **1984**, *81*, 3684–3690.
- Carignano, M. A.; Szeleifer, I. *J. Chem. Phys.* **1995**, *102*, 8662–8669.
- Szeleifer, I. *Curr. Opin. Colloidal Interface Sci.* **1996**, *1*, 416–423.
- Szeleifer, I. *Curr. Opin. Solid State Mater. Sci.* **1997**, *2*, 337–344.
- Charlier, J.-C.; Iijima, S. Growth Mechanisms of Carbon Nanotubes. In *Carbon Nanotubes*; Dresselhaus, M. S., Dresselhaus, G., Avouris, Ph., Eds.; Topics in Applied Physics 80; Springer-Verlag: Berlin and Heidelberg, Germany, 2001; p 55.
- O'Connell, M. J.; Bachilo, S. M.; Huffman, C. B.; Moore, V. C.; Strano, M. S.; Haroz, E. H.; Rialon, K. L.; Boul, P. J.; Noon, W. H.; Ma, J.; Hauge, R. H.; Weisman, R. B.; Smalley, R. E. *Science* **2002**, *297*, 593.
- Liu, L.; Barber, A. H.; Nuriel, S.; Wagner, D. H. *Adv. Funct. Mater.* **2005**, *15*, 975–980.
- TEM and Cryo-TEM images clearly show that the tubes are exfoliated into individual tubes and small bundles. A thorough investigation of the effect of exfoliation of HiPCO SWNT on the Raman spectra was carried out by Izard et al.<sup>59</sup> They as well, do not observe a change in the Raman spectra of suspended and exfoliated SWNT as compared to the bundled powder.
- Izard, N.; Rieh, D.; Anglaret, E. *Phys. Rev. B* **2005**, *71*, 195417.
- Jorio, A.; Pimenta, M. A.; Souza Filho, A. G.; Saito, R.; Dresselhaus, G.; Dresselhaus, M. S. *New J. Phys.* **2003**, *5*, 139.
- Lefrant, S.; Baltog, I.; Baibarac, M. *J. Raman. Spectrosc.* **2005**, *36*, 676–698.

- (63) Wanaka, G.; Hoffman, H.; Ulbricht, W. *Macromolecules* **1994**, *27*, 4145–4159.
- (64) Lopes, J. R.; Loh, W. *Langmuir* **1998**, *14*, 750–756.
- (65) Alexandridis, P.; Holzwarth, J. F.; Hatton, T. A. *Macromolecules* **1994**, *27*, 2419.
- (66) Polat, H.; Chander, S. *Colloids Surf. A* **1999**, *146*, 199–212.
- (67) Lin, Y.; Alexandridis, P. *J. Phys. Chem. B* **2002**, *106*, 10834.
- (68) Alexandridis, P.; Athanassiou, V.; Fukuda, S.; Hatton, T. A. *Langmuir* **1994**, *10*, 2604.
- (69) Camponeschi, E. B.; Vance, R.; Garrett, G.; Garmestani, H.; Tannenbaum, R. *Langmuir* **2006**, *22*, 1858–62.
- (70) Fischer, H. *Mater. Sci. Eng. C* **2003**, *23*, 763.
- (71) Yerushalmi – Rozen, R.; Szeifer, I. *Soft Matter* **2006**, *2*, 24–28.
- (72) Wool, R. P. In *Handbook of Adhesion*, 2nd ed.; Packham, D. E., Ed.; Wiley: West Sussex, England, 2006; p 341.
- (73) Nap, R.; Szeifer, I. *Langmuir* **2005**, *21*, 12072–12075.
- (74) Dror, Y.; Pyckhout Hintzen, W.; Cohen, Y. *Macromolecules* **2005**, *38*, 7828–7836.
- (75) Two very different types of amphiphilic polymers were examined in this study: an alternating copolymer of styrene (hydrophobic) and sodium maleate (hydrophilic) and a highly branched natural polysaccharide, gum arabic.
- (76) Szeifer, I.; Carignano, M. A. *Macromol. Rapid Commun.* **2000**, *21*, 423–448.
- (77) Polymer adsorption is characterized by a high affinity curve where the adsorption plateau is reached at a low bulk concentration: Fler, G. J.; Cohen Stuart, M. A.; Scheutjens, J. H. M.; Cosgrove, T. *Polymers at Interfaces*; Chapman and Hill: London, 1993.
- (78) The adsorption isotherms of different Pluronics onto carbon black were found to exhibit a high affinity curve where the adsorption plateau is reached at a bulk concentration much smaller than the cmc.<sup>67</sup>

MA0705366